ISSN 1990-7931, Russian Journal of Physical Chemistry B, 2010, Vol. 4, No. 6, pp. 995–1004. © Pleiades Publishing, Ltd., 2010.
Original Russian Text © V.Ya. Basevich, A.A. Belyaev, S.N. Medvedev, V.S. Posvyanskii, F.S. Frolov, S.M. Frolov, 2010, published in Khimicheskaya Fizika, 2010, Vol. 29, No. 12, pp. 50–59.

COMBUSTION, EXPLOSION, AND SHOCK WAVES

Simulation of the Autoignition and Combustion of *n*-Heptane Droplets Using a Detailed Kinetic Mechanism

V. Ya. Basevich, A. A. Belyaev, S. N. Medvedev, V. S. Posvyanskii, F. S. Frolov, and S. M. Frolov

Semenov Institute of Chemical Physics, Russian Academy of Sciences, Moscow, 119991 Russia

e-mail: basevich@center.chph.ras.ru

Received June 9, 2010

Abstract—The autoignition and combustion of *n*-heptane droplets are simulated using a detailed kinetic mechanism. A mathematical model, based on first principles, contains no adjustable parameters. The burning rate constants for the combustion of droplets are calculated over a wide range of pressures, temperature, fuel-to-oxidizer equivalence ratios of the gas–droplet suspension, and droplet diameters. The calculated and measured delay times of autoignition of droplets are compared. The calculation results agree well with the available experimental data. The detonability of gas–droplet suspensions with partial pre-evaporation of fuel is estimated.

Keywords: *n*-heptane combustion, autoignition of droplets, mathematical model, detonability.

DOI: 10.1134/S1990793110060187

INTRODUCTION

It is known that *n*-heptane, as a representative of the homologous series of normal alkanes, exhibits a multistage low-temperature autoignition due to the existence of competing mechanisms of chain branching. The multistage ignition of homogeneous *n*-heptane–air mixtures occurs as a sequence of cool, blue, and hot flames [1]. The acceleration of the reaction in the cool flame is a consequence of chain branching during the decomposition of alkyl hydroperoxide (here, heptyl hydroperoxide $C_7H_{15}O_2H$) with the formation of a hydroxyl and an alkyloxy radical. A blue flame arises because of chain branching during the decomposition of hydrogen peroxide H_2O_2. Hot explosion is a consequence of a branched-chain reaction of atomic hydrogen with molecular oxygen. One of the most striking features of multistage autoignition is the existence of a region with a negative temperature coefficient (NTC) of the reaction rate, when at a higher initial temperature, the total ignition delay time is longer than that at a low temperature.

Methods of modern mathematical theory of combustion makes it possible to calculate the characteristics of the autoignition and laminar combustion of gaseous mixtures of *n*-heptane on the basis of first principles, i.e., without introducing adjustment coefficients and to obtain a satisfactory agreement with experimental data. Such calculations are performed using detailed kinetic mechanisms (DKMs) of fuel oxidation and databases of thermophysical properties of substances (see, e.g., [2, 3]).

As for the ignition and subsequent burning of *n*-heptane droplets, simulations of these processes are mainly based on empirical [4–8] or semiempirical [9–11], kinetic mechanisms.

In [4, 5], the high-temperature autoignition and combustion of single droplets of *n*-heptane and of homogeneous monodisperse gas–droplet suspensions were described within the framework of an empirical mechanism composed of 10 reactions involving 10 components: C_7H_{16}, O_2, N_2, CO, CO_2, H_2, H_2O, NO, soot S, and a generalized radical R. The mechanism was tested by applying it to describing the high-temperature autoignition of premixed gas mixtures, the propagation of a laminar flame in such a gas, and the counterflow diffusion combustion of gases. In [6], this mechanism was used to determine the conditions for the existence of a heterogeneous detonation in gas–droplet suspensions of *n*-heptane, whereas in [7, 8], to calculate the structure and limits of the heterogeneous detonation of gas– droplet suspensions.

In [9], the autoignition of single *n*-heptane droplets was simulated using the semiempirical kinetic mechanism from [12], which includes both high- and low-temperature reactions, which simulate the NTC of the reaction rate in a homogeneous mixture. However, the authors of [9] revealed no NTC region while simulating the low-temperature autoignition of droplets. Numerical simulations of the low-temperature autoignition of single *n*-heptane droplets with the use of a semiempirical mechanism containing 62 reactions were performed in [10]. In contrast to [9], in the calculations [10], an NTC region was detected, but as compared to the experimental data, it turned out to be significantly shifted toward lower temperatures. In [11], the high-temperature autoignition of single

n-heptane droplets was simulated using a semiempirical mechanism composed of 282 and 51 components.

The main drawback of semiempirical mechanisms is that their applicability to the specific conditions of calculations should be tested using experimental data. However, since experimental data are usually scarce, these mechanisms are often extrapolated to a region of governing parameters in which such tests have not been conducted.

At present, only in rare cases, autoignition and combustion of *n*-heptane droplets are investigated using DKMs. In [13], on the basis of a DKM including 904 reactions and 168 components, simulations of the low-temperature autoignition delays in a three-dimensional two-phase turbulent flow with monodisperse droplets of *n*-heptane were performed. Owing to the large computational cost, the modeling of associated physical processes was significantly simplified: the temperature distribution over the droplet and the computational grid cell, whose size is many times the diameter of the droplet, was assumed uniform. In fact, the authors of [13] simulated the gas-phase low-temperature autoignition of *n*-heptane with some averaged parameters of the evaporation of the liquid.

In [14], a numerical simulation of forced ignition and combustion of single *n*-heptane droplets in a $25\%O_2 + 75\%$He atmosphere with the use of the block of reactions from a DKM of *n*-decane oxidation containing 5000 reactions involving 200 components. The focus was on the sensitivity of the conditions of extinction of the flame around the droplet to changes in the governing parameters of the problem.

Note that, in none of the cited works on the mathematical modeling of the ignition and combustion of droplets of *n*-heptane, a blue flame was observed, and even the possibility of its existence was not discussed. In addition, all attempts to take into account collective effects in gas–droplet suspensions were reduced to averaging the temperature and concentration of fuel vapor in the space between the droplets. Meanwhile, other, more accurate approaches to the collective effects in gas–droplet suspensions have been described in the literature. For this purpose, a multidimensional problem for two or more droplets [15, 16], a regular array of droplets [17, 18], or a group of randomly spaced droplets [19, 20] is solved, or a one-dimensional spherically symmetric problem for a single droplet with the boundary conditions of screening of mass and energy fluxes at the mid-distance between particles in a homogeneous monodisperse gas–droplet suspension [21, 22] is considered.

The aim of this work was to numerically simulate the autoignition and combustion of single *n*-heptane droplets, as well as homogeneous monodisperse droplet–gas mixtures using a nonempirical model of heating, evaporation, autoignition and combustion of droplets [4, 5, 21, 22] in conjunction with a DKM for fuel oxidation [3]. The main purpose of the model is to refine the estimates of the detonability of air–*n*-heptane droplet mixtures obtained in [6–8]. Such estimates are important for the development of safety measures to prevent accidental explosions, as well as to optimize the performance of liquid fuel air-breathing pulse detonation engine [23].

The spherically symmetric model described in [4, 5, 21, 22] is based on nonstationary differential equations of conservation of mass and energy in the liquid and gas phases with variable thermophysical properties. In formulating the problem, the concept of multicomponent diffusion in the gas phase was used. The model was constructed for the conditions of microgravity and constant pressure in the gas–droplet system. An important advantage of the DKM from [3] is that it describes both the multistage, low-temperature oxidation in the cool- and blue-flame modes and the high-temperature combustion of *n*-heptane and that it does not require additional testing.

MODEL

The mathematical model of heating, evaporation, autoignition, and combustion of droplets was based on the following equations [21, 22].

The continuity equation for the liquid $(0 < r < r_m)$:

$$\frac{\partial \rho_d}{\partial t} + \frac{1}{r^2}\frac{\partial}{\partial r}\left(r^2 \rho_d u_d\right) = 0, \tag{1}$$

where r_m is the droplet radius, t is the time, r is the radial coordinate, $\rho_d(T_d)$ is the density of the liquid, and u_d is the velocity of the liquid.

The energy conservation equation for the liquid $(0 < r < r_m)$:

$$c_d \rho_d \frac{\partial T_d}{\partial t} + c_d \rho_d u_d \frac{\partial T_d}{\partial r} = \frac{1}{r^2}\frac{\partial}{\partial r}\left(\lambda_d r^2 \frac{\partial T_d}{\partial r}\right),$$
$$T_d(0,r) = T_{d0}, \quad \left.\frac{\partial T_d}{\partial r}\right|_{r=0} = 0, \tag{2}$$
$$T_d(t,r_m) = T_g(t,r_m),$$

where $T_d = T_d(r, t)$ is the temperature of the liquid, $c_d(T_d)$ is the specific heat of the liquid, $\lambda_d(T_d)$ is the thermal conductivity of the liquid, the subscripts 0 and g hereafter refer to the initial values and the parameters of the gas around the droplet.

The equation for the mass concentration of vapor of the liquid at the droplet surface $(r = r_m)$:

$$Y_v = \frac{P_v}{P}\frac{W_v}{\overline{W}}, \tag{3}$$

where P is the pressure, W is the molecular mass (the overbar denotes the quantity being averaged), and the subscript v refers to the vapor of the liquid.

The continuity equation for the gas phase ($r_m < r < R$):

$$\frac{\partial \rho_g}{\partial t} + \frac{1}{r^2}\frac{\partial}{\partial r}(r^2 \rho_g u_g) = 0,$$
$$\rho_d\left(V_d - \frac{\partial r_m}{\partial t}\right)\Big|_{r=r_m} = \rho_g\left(u_g - \frac{\partial r_m}{\partial t}\right)\Big|_{r=r_m}, \quad (4)$$

where R is the radius of the computational domain around the droplet (characterizes the mid-distance between neighboring droplets in the gas suspension) and the derivative $\partial r_m/\partial t$ determines the instantaneous velocity of the droplet surface due to evaporation and thermal expansion.

The equation of continuity of the gaseous components ($r_m < r < R$):

$$\rho_g \frac{\partial Y_j}{\partial t} = \frac{1}{r^2}\frac{\partial}{\partial r}(\rho_g r^2 Y_j V_j) - \rho_g u_g \frac{\partial Y_g}{\partial r} + \omega_{gj},$$
$$Y_j(0,r) = Y_{j0} \quad j = 1, 2, \ldots, N,$$
$$-\rho_d u_i \beta_j\big|_{r=r_m} = \rho_g Y_j\left(u_g - \frac{\partial r_m}{\partial t}\right) + \rho_g Y_j V_j\Big|_{r=r_m}, \quad (5)$$
$$\frac{\partial \bar{W} Y_j}{\partial r}\Big|_{r=R} = 0, \quad j = 1,\ldots,N,$$

where V_j is the diffusion velocity of the jth component, $u_i = u_i(t)$ is the velocity of movement of the droplet surface due to evaporation (note that there is another component of the droplet surface velocity due to thermal expansion of liquid). The initial mass concentrations Y_{j0} are specified in the form of uniform distributions in the gas phase. The rates of chemical reactions ω_{gj} and the coefficients β_j read as

$$\omega_{gj} = W_{gj}\sum_{k=1}^{L}(\nu''_{j,k} - \nu'_{j,k})A_k T_g^{n_k}\exp\left(-\frac{E_k}{RT_g}\right)\prod_{l=1}^{N}\left(\frac{Y_{gl}\rho_g}{W_{gl}}\right)^{\nu'_{l,k}},$$
$$\beta_j = 1 \text{ at } j = v,$$
$$\beta_j = 0 \text{ at } j \neq v,$$

where A_k, n_k, and E_k are the preexponential factor, the temperature exponent, and activation energy for the kth reaction; $\nu'_{j,k}$ and $\nu''_{j,k}$ are the stoichiometric coefficients for the jth component in the case when it is a reactant and product in the kth reaction, respectively.

The equation for the diffusion velocity in the gas phase ($r_m < r < R$):

$$\frac{\partial X_j}{\partial r} = \sum_{k=1}^{N}\left(\frac{X_j X_k}{D_{jk}}\right)(V_k - V_j), \quad (6)$$

where $X_j = Y_j\bar{W}/W_j$ is the mole fraction of the jth component in the mixture.

The equations of conservation of energy in the gas phase ($r_m < r < R$):

$$c_{pg}\rho_g \frac{\partial T_g}{\partial t} = \frac{1}{r^2}\frac{\partial}{\partial r}\left(\lambda_g r^2 \frac{\partial T_g}{\partial r}\right) - c_{pg}\rho_g u_g \frac{\partial T_g}{\partial r} + \Omega,$$
$$T_g(0,r) = T_{g0}, \quad (7)$$
$$T_g(t,r_m) = T_d(t,r_m), \quad \frac{\partial T_g}{\partial r}\Big|_{r=R} = 0,$$

where $c_{pg} = c_{pg}(T_g)$, $\rho_g = \rho_g(p,T_g)$, $\lambda_g(p,T_g)$ are, respectively, the specific heat, density, and thermal conductivity of the gas mixture.

The chemical source of Ω in (7) is given by

$$\Omega = \sum_{k=1}^{L} H_k A_k T_g^{n_k}\exp\left(-\frac{E_k}{RT_g}\right)\prod_{j=1}^{N}\left(\frac{Y_{gj}\rho_g}{G_{gj}}\right)^{\nu'_{j,k}},$$

where H_k is the thermal effect of the kth chemical reaction.

The boundary condition of matching Eqs. (2) and (7) at the droplet surface ($r = r_m$) for determining the droplet surface temperature T_{di}:

$$\lambda_d \frac{\partial T_d}{\partial r} - \frac{\rho_{di} u_i L_v}{W_v} = \lambda_g \frac{\partial T_g}{\partial r}, \quad (8)$$

where the L_v is the latent heat of vaporization of the liquid.

The equation of state of an ideal gas for the gas phase:

$$\rho_g = \frac{P\bar{W}}{RT_g}. \quad (9)$$

The condition of pressure constancy:

$$P = \text{const}. \quad (10)$$

The system of equations (1)–(10), supplemented by a database of the thermophysical properties of the components [21, 22], was integrated numerically using a nonconservative implicit finite difference scheme and an adaptive moving grid. To calculate the chemical sources ω_{gj} and Ω, we used the DKM from [3], which included 83 components and 623 reversible reactions. The calculation procedure consisted of successive approximations at each time step. An important feature of the algorithm was a complete linearization of the conditions of matching of the solution at the droplet surface. The accuracy of the solution was continuously checked for compliance with the elemental balance of C and H atoms, as well as with energy balance.

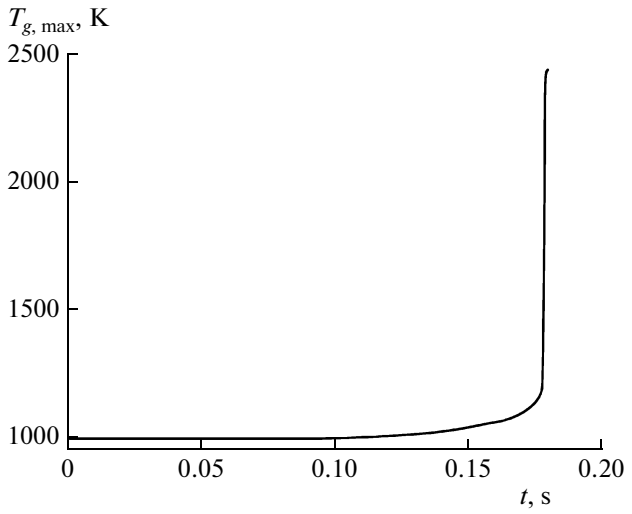

Fig. 1. Calculated time dependence of the maximum temperature $T_{g,\max}$ of the gas around an *n*-heptane droplet during its autoignition: $d_0 = 700$ μm, $T_{g0} = 1000$ K, $P =$ 1 atm, and $\Phi = 0.46$.

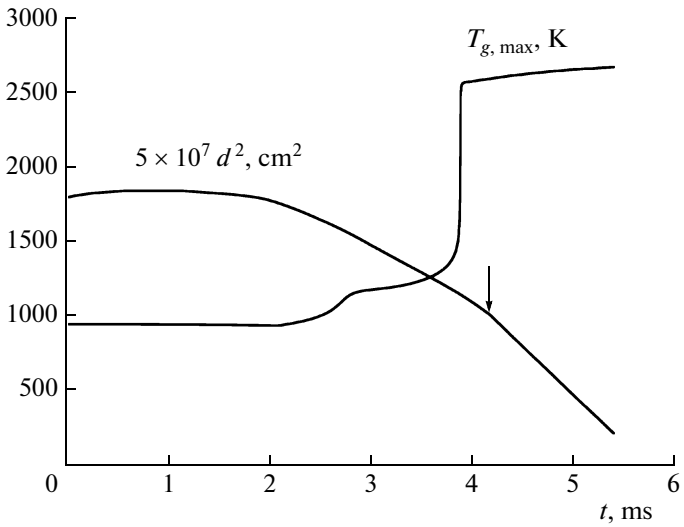

Fig. 2. Calculated time dependences of the maximum temperature $T_{g,\max}$ of the gas around an *n*-heptane droplet and of the square of its diameter during autoignition: $d_0 =$ 60 μm, $T_{g0} = 950$ K, $P = 20$ atm, and $\Phi = 1$.

CALCULATIONS OF THE AUTOIGNITION OF DROPLETS

To test the predictive ability of model (1)–(10) supplemented by the DKM for the ignition and combustion of *n*-heptane, we first calculated the delay time for the ignition of single quiescent *n*-heptane droplets in air and compared the calculated values of the induction period measured under microgravity [24, 25]. We assumed that, at the initial moment of time, the air around the droplet was uniformly heated to T_{g0} whereas the initial temperature of the liquid was $T_{d0} =$ 293 K. The radius R of the computational domain around the droplet was set sufficiently large compared to the initial radius of the droplet r_{m0}, so that, in the process of ignition, the physical parameters at the boundary of the domain did not change. Note that, in accordance with [21], any chosen value of R corresponds to a particular value of the fuel-to-oxidizer equivalence ratio Φ in a homogeneous monodisperse gas–droplet suspension:

$$R = r_m \left(\frac{\rho_d}{\rho_g \Phi \phi_{st}} \right)^{1/3}, \qquad (11)$$

where ϕ_{st} is the mass fraction of fuel in a stoichiometric mixture (for an air–*n*-heptane mixture, $\phi_{st} \approx 0.062$).

After a certain period, the induction period or the ignition delay time τ_i, the gas mixture autoignited at a certain distance from the surface of the droplet. Figure 1 shows the calculated dependence of the maximum temperature of the gas $T_{g,\max}$ on the time t for an *n*-heptane droplet with an initial diameter of $d_0 = 2r_{m0} = 700$ μm at an initial temperature of the air of $T_{g0} = 1000$ K and a pressure of 1 atm. The radius of the computational sphere R around the droplet corresponded to a fuel-to-oxidizer equivalence ratio of $\Phi =$ 0.46. In the calculations, the induction period τ_i was defined as the time interval from the beginning of the process to the point of intersection of two straight lines tangent to the temperature curve: parallel the time axis and passing through the inflection point. The table compares the calculated values of τ_i with the values measured in [24, 25]. Given the complexity of the physical and chemical processes around the droplet, the results appear to be satisfactory.

Autoignition delay time for single *n*-heptane droplets at a pressure of 1 atm

Initial droplet diameter, μm	Air temperature, K	Autoignition delay time, s	
		experiment	calculation
700	1000	0.30 [24]	0.18
1000	960	0.58 [25]	0.27

CALCULATIONS OF THE COMBUSTION OF DROPLETS

Next, we addressed to the problem of the autoignition and subsequent combustion of spherical *n*-heptane droplets with different sizes over a wide range of conditions in pressure P, temperature T_{g0} and fuel-to-oxidizer equivalence ratio Φ.

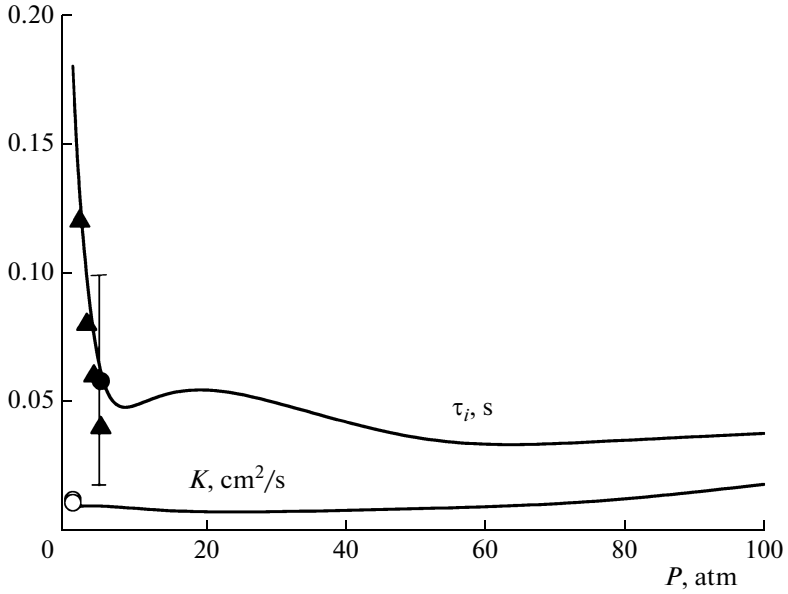

Fig. 3. Calculated pressure dependences of the autoignition delay time τ_i and the burning rate constant K for an n-heptane droplet with $d_0 = 700$ μm at $T_{g0} = 1000$ K and $\Phi = 1$. The closed symbols represent the measured values of τ_i for single n-heptane droplets ($\Phi \to 0$): (triangles) $d_0 = 700$–750 μm [26] and (circles) $d_0 = 700$ μm and $T_{g0} = 940$ K [10] (the vertical bar indicates the scatter in experimental data). Open symbols represent measured values of K for single n-heptane droplets ($\Phi \to 0$): (circles) $d_0 = 700$–1700 μm and $T_{g0} = 973$ K [27].

The calculations showed that, at certain pressures and temperatures, the autoignition of n-heptane droplets occurs as a multistage process, well known for gas-phase oxidation. For example, the $T_{g,\max}(t)$ curve in Fig. 2 illustrates the multistage autoignition of a $d_0 = 60$ μm droplet at $P = 20$ atm and $T_{g0} = 950$ K. The multistage character of the process manifests itself as a stepped increase in the temperature within 2.5–3.0 ms due to the blue flame associated with the decomposition of accumulated hydrogen peroxide [3] (the total induction period of autoignition is ~3.87 ms). That multistage nature of the process clearly manifests itself is largely due to the gas suspension assumed to be monodisperse. At certain values of temperature T_{g0} and pressure P, the multistage character manifested in the form of successive cool and blue flames, preceding a hot explosion in the gas phase. Obviously, for a real polydisperse spray, such stepwise increases in temperature are not registered because of a strong dependence of the physical and chemical processes around the droplets on their size and spatial distribution. However, locally, the multistage ignition always takes place.

After the hot explosion, the droplet starts to burn. First, at some distance from the droplet surface, a high-temperature flame is formed, and then the flame temperature reaches a steady-state value, i.e., the period of steady burning of the droplet sets in. Using the rate of decrease of the square of the droplet diameter, one can determine the constant K in the burning rate law constant:

$$d^2 = d_0^2 - Kt, \qquad (12)$$

where d is the droplet diameter at time t. In fact, the $d^2(t)$ dependence is more complicated than linear dependence (12). An example of the calculated $d^2(t)$ dependence is shown in Fig. 2. As can be seen, after a small initial increase in the droplet diameter (caused by the thermal expansion of the liquid: the maximum value is $d^2 = 3.69 \times 10^{-5}$ cm^2 instead of the initial value of 3.60×10^{-5} cm^2), it decreases due to evaporation, and then, after the ignition of fuel vapor (this moment is shown by the arrow), it decreases at a higher rate. Over this last portion of the $d^2(t)$ curve, its slope remains approximately constant and equal to the burning rate constant K, which is defined by the current value of $T_{\max}$.

It is interesting to examine how the ignition delay time and the burning rate constant of droplets depend on the pressure P. As an example, Fig. 3 shows the results of calculations at $d_0 = 700$ μm, $T_{g0} = 1000$ K, and $\Phi = 1$ (τ_i and K curves). The τ_i curve in Fig. 3 shows the calculated $\tau_i(P)$ dependence within 1–100 atm. As can be seen, the ignition delay time increases sharply at low pressures. The closed symbols in Fig. 3 correspond to the experimental data on the autoignition of single n-heptane droplets [10, 26]. In contrast, the $K(P)$ dependence in Fig. 3 is relatively

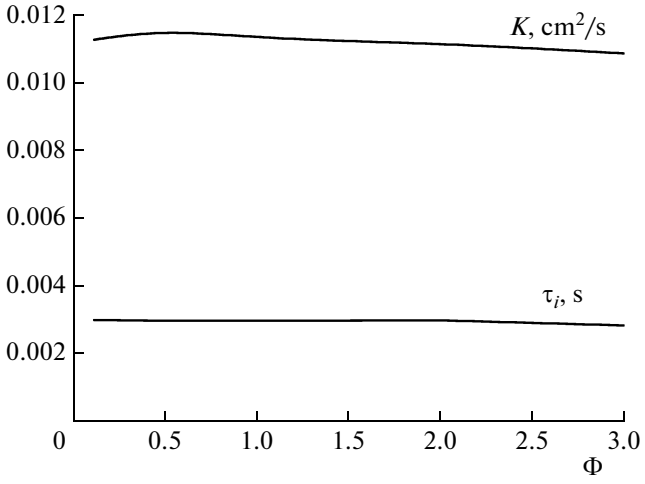

Fig. 4. Calculated dependences of the ignition delay time τ_i and burning rate constant K of an n-heptane droplet on the fuel-to-oxidizer equivalence ratio Φ for a gas–droplet suspension at $d_0 = 60$ μm, $T_{g0} = 1000$ K, and $P = 20$ atm.

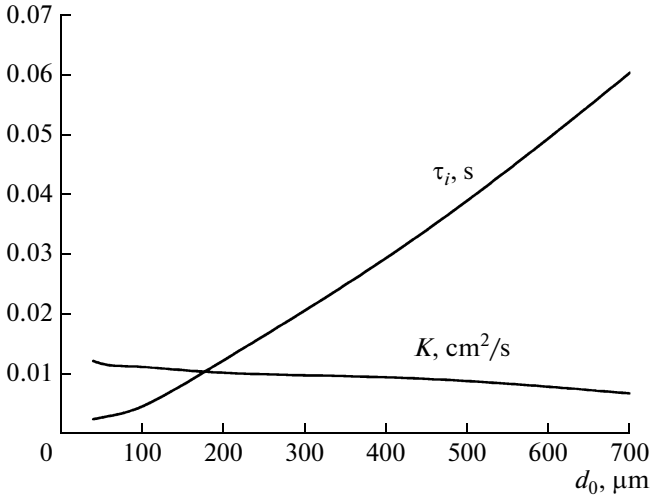

Fig. 5. Calculated dependences of the ignition delay time τ_i and burning rate constant K of an n-heptane droplet on the initial droplet diameter d_0 at $T_{g0} = 1000$ K, $P = 20$ atm, and Φ = 1.

weak: with increasing pressure K does so only slightly. The open symbols in Fig. 3 represent the experimental data reported in [27]. In general, the calculation results and experimental data for τ_i and K appear to be in close agreement.

Figure 4 shows the calculated dependences of τ_i and K on the initial value of the fuel-to-oxidizer equivalence ratio Φ in the gas suspension at $d_0 = 60$ μm, $T_{g0} = 1000$ K and $P = 20$ atm. It is seen that the $\tau_i(\Phi)$ and $K(\Phi)$ dependences are very weak.

Note that the calculations were performed only at $\Phi < 3$, when the mid-distance R between the droplets in the gas suspension is still large enough: at $\Phi = 3$ according to (11) $R/r_m \approx 7$. However, when simulating the combustion of gas mixtures highly rich in fuel, it is necessary to take into account the formation of soot and fuel pyrolysis products, as well as heat transfer by radiation, effects disregarded in model (1)–(10).

Figure 5 shows the calculated dependences of τ_i and K on the initial diameter of droplets d_0 in the gas mixture of stoichiometric composition ($\Phi = 1$) at $T_{g0} = 1000$ K and $P = 20$ atm. While the $\tau_i(d_0)$ dependence does not cause problems: in the case of small droplets, the fuel-air mixture is formed faster, the $K(d_0)$ dependence, at first glance, contradicts expression (12).

Recall, however, that expression (12) ignores the collective effects in a gas mixture of stoichiometric composition, whereas the calculated $K(d_0)$ dependence was obtained subject to conditions of zero mass and energy fluxes at the boundary of the computational domain R.

To determine the Arrhenius parameters (preexponential factor A_k and activation energy E_k) of elementary gas-phase reactions or some overall processes, the logarithm of the induction period of autoignition is normally plotted as a function of the reciprocal temperature T_{g0}^{-1}. Despite the fact that the autoignition and combustion of droplets occurs in the gas phase, the chemical process is complicated by the evaporation of liquid, thermal conductivity, mutual diffusion of fuel, oxidizer, intermediates, and final products, as well as by convective (Stephan) flow. Nevertheless, by constructing the $\log\tau_i - T_{g0}^{-1}$ dependence, one can determine effective (macrokinetic) Arrhenius parameters for the process of autoignition of droplets. As can be seen from Fig. 6, at $P = 20$ atm, $\Phi = 1$, and $d_0 = 60$ μm, the calculated $\log\tau_i - T_{g0}^{-1}$ dependence for n-heptane droplets is an S-shape, even though weakly expressed. The same shape, but more pronounced, is typical of the gas-phase oxidation of n-heptane under homogeneous conditions [3, 12]. An inspection of Fig. 6 shows that, at $P = 20$ atm, $\Phi = 1$, and $d_0 = 60$ μm, the effective activation energy E_e in the high-temperature region for the autoignition of droplets is ~18 kcal/mol and ~8 kcal/mol at low temperatures. The symbols in Fig. 6 represent the measurements from [28] (cited in the review [29]). In [28], the ignition induction period was measured by injecting a liquid n-heptane spray into an electrically heated furnace. The moment of ignition was identified with the appearance of glow.

Figure 7 displays the calculated dependence of the burning rate constant K for an n-heptane droplet as a function of the ambient air temperature T_{g0} at $P = 20$ atm, $\Phi = 1$ and $d_0 = 60$ μm. It is seen that the

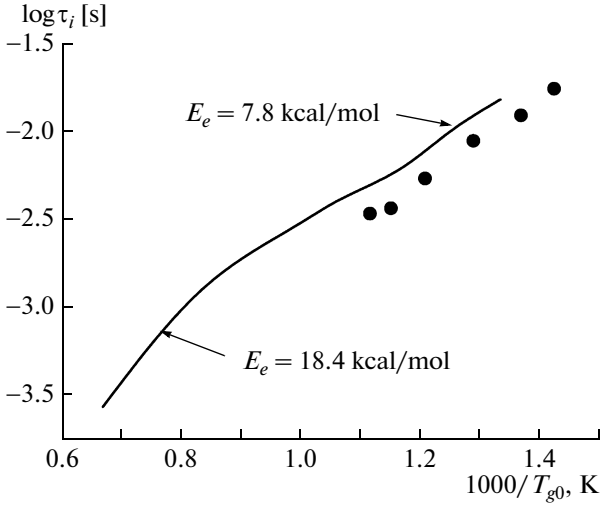

Fig. 6. Calculated dependence of the logarithm of the delay time of autoignition $\log\tau_i$ of a droplet on the reciprocal temperature T_{g0}^{-1}: $d_0 = 60$ μm, $P = 20$ atm, and $\Phi = 1$. The symbols represent the experimental data from [28] for $P = 21$ atm.

$K(T_{g0})$ dependence is nonmonotonic: at $T_{g0} \approx 985$ K, it passes through a maximum with $K \approx 0.013$ cm^2/s. Generally, within 800 K $\le T_{g0} \le$ 1500 K, the calculated K value varies from 0.008 cm^2/s at 800 K to 0.013 cm^2/s at 985 K, and to 0.01 cm^2/s at 1500 K. Note that, for the conditions used to plot the graphs presented in Figs. 1–7, there is only a limited number of experimental data concerning K. However, the available published experimental data for *n*-heptane at different values of T_{g0}, P, Φ, and d_0 yield $K = 0.0047$–0.0157 cm^2/s [30–34]. Since these calculated values of K are consistent with the results of measurements, one can conclude that model (1)–(10), supplemented by a DKM for the gas-phase oxidation of *n*-heptane, satisfactorily describes not only the ignition but also the combustion of droplets.

DETONATION OF *n*-HEPTANE DROPS IN THE AIR

Based on a model of the autoignition and combustion of *n*-heptane droplets with a semiempirical kinetic mechanism of oxidation, the authors of [6] examined under what conditions heterogeneous droplet detonation can occur. The analysis was based on a comparison of the characteristic times of heat release in gas and heterogeneous detonation waves. As a criterion of detonability, the reaction time of $t_* = 100$ μs was accepted, which approximately corresponds to the detonation limit for stoichiometric gaseous hydrocarbon–air mixtures at normal initial pressure. Calculations showed that whether the detonation of a heterogeneous droplet mixture is possible is largely determined by the presence of a sufficient amount of fuel in its vapor phase at the instant of initiation. If the initial fuel content is below a certain value, gas–*n*-heptane droplet mixture turns out to be nondetonable. For example, it was shown [6] that the conditions behind a shock wave leading the detonation of a uniform monodisperse stoichiometric ($\Phi = 1$) suspension with 8-μm-in-diameter *n*-heptane droplets and with a 75% initial fuel vapor content correspond to the detonation limit. In other words, at fuel vapor contents of 50, 25, and 0%, *n*-heptane droplets with a diameter of

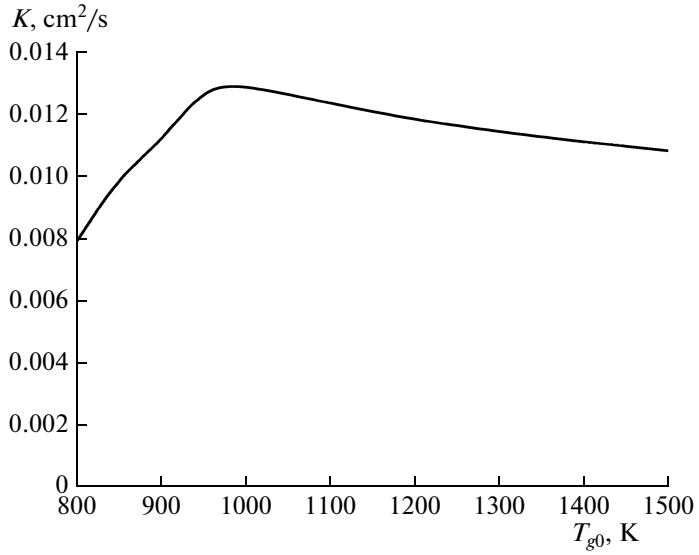

Fig. 7. Calculated dependence of the burning rate constant K for an *n*-heptane droplet on the initial temperature T_{g0} at $d_0 = 60$ μm, $P = 20$ atm, and $\Phi = 1$.

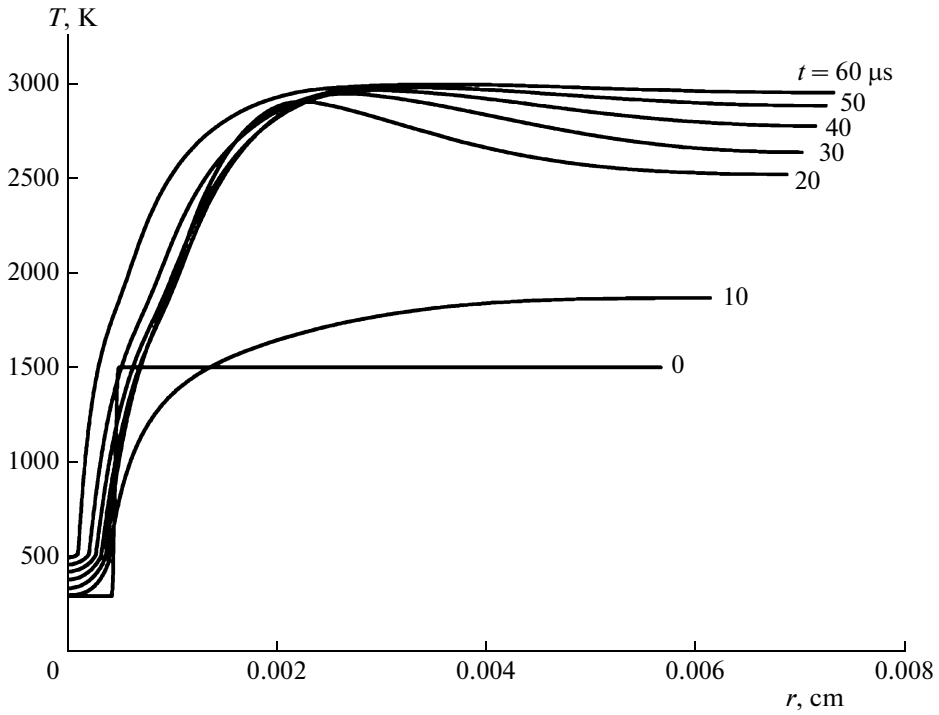

Fig. 8. Calculated spatial distribution of temperature over a droplet and around it at various moments of time at $d_0 = 7.9$ μm, $T_{g0} = 1500$ K, $P = 30$ atm, $\Phi = 1$, and $\Psi = 0.5$.

8 μm fail to fully react in time t_*; i.e., according to the above criterion, detonation is impossible. For example, at a 0, 25, and 50% vapor content in the gas phase, the amount of unreacted *n*-heptane at time t_* is 95%, 4.6%, and 2.5% respectively.

A refined model of heterogeneous droplet detonation was proposed in [7, 8]. The model considers the local autoignition and diffusion-limited combustion of the mixture around the droplets at variable averaged flow parameters behind the shock wave leading the detonation. It was shown [7, 8] that, given the strong sensitivity of heterogeneous detonation to the content of fuel in lean and near-stoichiometric mixtures, such mixtures apparently do not detonate.

To verify the conclusions drawn in [6–8], we performed here, calculations with the use of a DKM for *n*-heptane oxidation. As in [6], the conditions in the detonation wave were set identical to those characteristic of the von Neumann spike for detonation waves in mixtures of hydrocarbon fuels with air (the temperature and pressure behind the leading shock wave, $T_{g0} =$ 1500 K and $P = 30$ atm; the shock wave velocity, 1800 m/s). We assumed that the shock wave propagates in an *n*-heptane–air stoichiometric mixture, that the fuel in the mixture is partially vaporized, with the rest being present as a uniform monodisperse gas suspension of droplets of diameter d_0, and that the vapor content of the fuel in the gas phase is specified by degree of pre-evaporation of droplets Ψ. It was also postulated that in the absence of pre-evaporation of fuel, i.e., at $\Psi = 0$, the drops had a diameter $d_0 = 10$ μm.

As an example, Fig. 8 shows the calculated spatial distribution of temperature around a *n*-heptane droplet at different moments of time after the arrival of the shock wave. In this example, $\Psi = 0.5$ and $d_0 = 8$ μm. At the end of the induction period, at $\tau_i \approx 10$ μs, the preliminary prepared vapor–air mixture first ignites at a sufficiently large distance from the droplet, where there is no effects associated with the thermal and diffusion fluxes caused by its heating and evaporation. Then, the combustion wave reaches the nonuniform region in the immediate vicinity of the drop, where a high temperature diffusion flame forms and a local temperature maximum arises. Then, the drop completely burns out within $t \approx 60$ μs $< t_*$. According to the above criterion, a gas–droplet mixture of stoichiometric composition with $\Psi = 0.5$ and $d_0 \approx 8$ μm is detonable. Thus, the replacement of the semiempirical kinetic mechanism of *n*-heptane oxidation by the DKM resulted in an expansion of the detonability limits for 8-μm *n*-heptane droplets : instead of the limiting condition $\Psi \approx 0.75$, we obtained $\Psi \approx 0.5$.

Figure 9 shows the calculated dependence of the maximum gas temperature T_{max} and the square of the droplet diameter d^2 on the time at $\Psi = 0$ ($d_0 =$ 10 μm), 0.25 ($d_0 \approx 9$ μm), 0.50 ($d_0 \approx 8$ μm), and

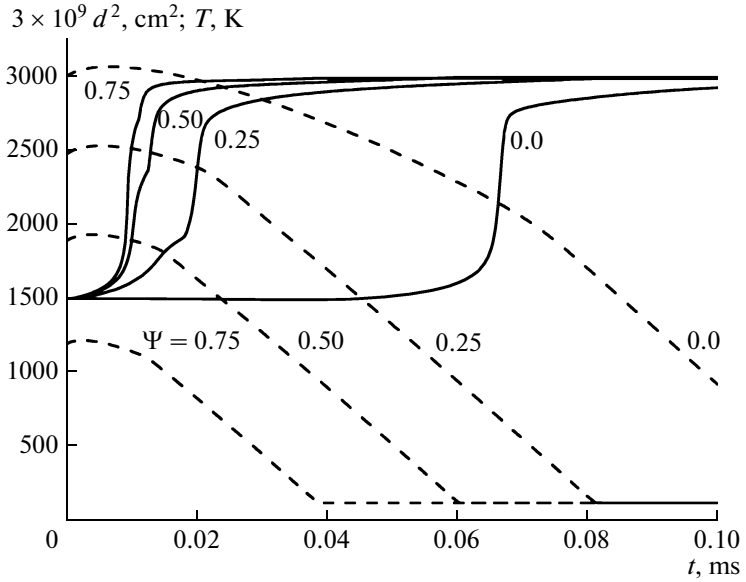

Fig. 9. Calculated time dependences of the maximum temperature T_{max} of the gas (solid lines) and the squared droplet diameter d^2 (dashed lines) at $T_{g0} = 1500$ K, $P = 30$ atm, $\Phi = 1$, and various degrees of pre-evaporation of droplets: $\Psi = 0$, 0.25, 0.50, and 0.75.

0.75 ($d_0 \approx 6$ μm). One can see that, at $\Psi = 0$, i.e., without partial evaporation (prior to the arrival of the shock wave), an *n*-heptane droplet with $d_0 = 10$ μm in a stoichiometric gas–droplet mixture does not have time to burn out within a time of $t_* = 100$ μs. In accordance with the accepted criterion, at $\Psi = 0$, detonation is impossible. In the other cases, i.e., at $\Psi = 0.25$, 0.5 and 0.75, gas–droplet mixtures are detonable.

The results obtained are confirmed by experimental studies (see, e.g., [35, 36]). In these works, the detonation of sprayed kerosene, JP-10 [35] and TS-1 [36], in the air was possible only due to a partial evaporation of the fuel (up to $\Psi = 0.75$).

CONCLUSIONS

The ignition and combustion of air–*n*-heptane droplet mixtures were simulated within the framework of a detailed kinetic mechanism. The model is constructed based on first principles, without invoking adjustable parameters. The ignition delay time and burning rate constant for *n*-heptane droplets were calculated over a wide range of pressures, temperatures, fuel-to-oxidizer equivalence ratios, and initial droplet diameters. We obtained refined estimates of the detonability of air–*n*-heptane mixtures at different degrees of fuel pre-evaporation.

The results obtained are in satisfactory agreement with experimental data and show a marked influence of chemical processes not only on the autoignition but also on diffusion combustion of droplets. The mathematical model can be used to determine the conditions for the existence and limits of the heterogeneous detonation in air–liquid fuel droplet mixtures.

ACKNOWLEDGMENTS

This work was supported by the Federal Program "Scientific and Scientific-Pedagogical Cadre of Innovative Russia for 2009–2013" (contract no. P502) and the Russian Foundation for Basic Research, project no. 08-08-00068.

REFERENCES

1. A. S. Sokolik, *Self-Ignition, Flame and Detonation in Gases* (Akad. Nauk SSSR, Moscow, 1960) [in Russian].
2. M. Nense and J. Warnatz, Proc. Combust. Inst. **26**, 773 (1996).
3. V. Ya. Basevich, A. A. Belyaev, and S. M. Frolov, Khim. Fiz. **29** (12), 41 (2010).
4. S. M. Frolov and V. Ya. Basevich, in *Laws of Combustion*, Ed. by Yu. V. Polezhaev (Energomash, Moscow, 2006), p. 130 [in Russian].
5. S. M. Frolov, V. Ya. Basevich, A. A. Belyaev, V. S. Posvyanskii, and V. A. Smetanyuk, in *Combustion and Pollution: Environmental Effect*, Ed. by G. D. Roy, S. M. Frolov, and A. M. Starik (Torus Press, Moscow, 2005), p. 117 [in Russian].
6. V. Ya. Basevich, S. M. Frolov, and V. S. Posvyanskii, Khim. Fiz. **24** (7), 60 (2005).
7. S. M. Frolov and V. S. Posvyanskii, in *Combustion and Explosion* (Torus Press, Moscow, 2008), No. 1, p. 1 [in Russian].
8. S. M. Frolov, in *Liquid Fragmentation in High-Speed Flow*, Ed. by P. Rambaud and C. O. Asma (Von Karman Inst. for Fluid Mechanics, Belgium, 2009), p. 1.

9. M. Tanabe, M. Kono, J. Sato, J. Koenig, C. Eigenbrod, F. Dinkelacker, and H. J. Rath, Combust. Sci. Technol. **108**, 103 (1995).
10. S. Schnaubelt, O. Moriue, T. Coordes, C. Eigenbrod, and H. J. Rath, Proc. Combust. Inst. **28**, 953 (2000).
11. A. J. Marchese, F. L. Dryer, and V. Nayagam, Combust. Flame **116**, 432 (1999).
12. J. F. Griffiths, Combust. Flame **93**, 202 (1993).
13. M. Cano Wolf, J. Meisl, R. Koch, and S. Wittig, Proc. Combust. Inst. **27**, 2025 (1998).
14. A. Cuoci, M. Mehl, G. Buzzi-Ferraris, T. Faravelli, D. Manca, and E. Ranzi, Combust. Flame **143**, 211 (2005).
15. E. M. Twardus and T. A. Brzustowski, Archiwum Process. Spalania **8**, 347 (1977).
16. H. A. Dwyer, H. Nirschl, P. Kerschl, and V. Denk, in *Proc. 25th Intern. Symp. on Combustion* (The Combust. Inst., Pittsburgh, PA, 1994), p. 389.
17. M. Marberry, A. K. Ray, and K. Leung, Combust. Flame **57**, 237 (1984).
18. K. Sivasankaran, K. N. Seetharamu, and R. Natarajan, Int. J. Heat Mass Transfer **39**, 3949 (1996).
19. H. H. Chiu and T. M. Liu, Combust. Sci. Technol. **17**, 127 (1977).
20. S. M. Correa and M. Sichel, in *Proc. 19th Intern. Symp. on Combustion* (The Combust. Inst., Pittsburgh, PA, 1983), p. 981.
21. S. M. Frolov, V. S. Posvyanskii, and V. Ya. Basevich, Khim. Fiz. **23** (4), 75 (2004).
22. S. M. Frolov, V. Ya. Basevich, and F. S. Frolov, Khim. Fiz. **28** (5), 3 (2009) [Russ. J. Phys. Chem. B **3**, 333 (2009)].
23. S. M. Frolov, *Pulse Detonation Engines* (Torus Press, Moscow, 2006) [in Russian].
24. M. Takei, H. Kobayashi, and T. Niioka, Int. J. Microgravity Res. Appl. Microgravity Sci. Technol. **6** (3), 184 (1993).
25. T. Niioka, H. Kobayashi, and D. Mito, in *Proc. IVTAM Symp. on Mechanics and Combust. of Droplets and Sprays* (Tainan, 1994), p. 367.
26. M. Tanabe, T. Bolik, C. Eigenbrod, and H. J. Rath, Proc. Combust. Inst. **26**, 1637 (1996).
27. K. Kobayasi, Proc. Combust. Inst. **5**, 141 (1955).
28. S. Ikura, T. Kadota, and H. Hiroyasu, Trans. Japan Soc. Mech. Engrs. **41**, 1559 (1981).
29. S. K. Aggarval, Prog. Energy Combust. Sci. **24**, 565 (1998).
30. J. A. Bolt and T. A. Boyle, Trans. ASME **78**, 609 (1956).
31. M. Goldsmith, Jet Propulsion **26**, 172 (1956).
32. J. F. Rex, A. E. Fuhs, and S. S. Penner, Jet Propulsion **26**, 179 (1956).
33. S. Kumagai, Jet Propulsion **26**, 786 (1956).
34. J. Kanevsky, Jet Propulsion **26**, 788 (1956).
35. C. M. Brophy, D. W. Netzer, et al., in *High-Speed Deflagration and Detonation*, Ed. by G. Roy, S. Frolov, et al. (Elex-KM, Moscow, 2001), p. 207.
36. S. M. Frolov and V. S. Aksenov, Dokl. Akad. Nauk **416** (3), 1 (2007).